AAC
Journals.ASM.org

Limited Activity of Clofazimine as a Single Drug in a Mouse Model of Tuberculosis Exhibiting Caseous Necrotic Granulomas

Scott M. Irwin,[a] Veronica Gruppo,[a] Elizabeth Brooks,[a] Janet Gilliland,[a] Michael Scherman,[a] Matthew J. Reichlen,[b] Rachel Leistikow,[b] Igor Kramnik,[c] Eric L. Nuermberger,[d] Martin I. Voskuil,[b] Anne J. Lenaerts[a]

Mycobacteria Research Laboratories, Department of Microbiology, Immunology and Pathology, Colorado State University, Fort Collins, Colorado, USA[a]; University of Colorado School of Medicine, Department of Microbiology, Aurora, Colorado, USA[b]; Boston University School of Medicine, Department of Pulmonary, Allergy, Sleep and Critical Care Medicine, Boston University, Boston, Massachusetts, USA[c]; Center for Tuberculosis Research, Department of Medicine, Johns Hopkins University School of Medicine, Baltimore, Maryland, USA[d]

New drugs and drugs with a novel mechanism of action are desperately needed to shorten the duration of tuberculosis treatment, to prevent the emergence of drug resistance, and to treat multiple-drug-resistant strains of *Mycobacterium tuberculosis*. Recently, there has been renewed interest in clofazimine (CFZ). In this study, we utilized the C3HeB/FeJ mouse model, possessing highly organized, hypoxic pulmonary granulomas with caseous necrosis, to evaluate CFZ monotherapy in comparison to results with BALB/c mice, which form only multifocal, coalescing cellular aggregates devoid of caseous necrosis. While CFZ treatment was highly effective in BALB/c mice, its activity was attenuated in the lungs of C3HeB/FeJ mice. This lack of efficacy was directly related to the pathological progression of disease in these mice, since administration of CFZ prior to the formation of hypoxic, necrotic granulomas reconstituted bactericidal activity in this mouse strain. These results support the continued use of mouse models of tuberculosis infection which exhibit a granulomatous response in the lungs that more closely resembles the pathology found in human disease.

The Stop TB Partnership, in conjunction with the World Health Organization, has set a goal of reducing tuberculosis (TB) incidence to less than one case per million by 2050 (1). If we hope to achieve this goal, we must more effectively employ the current resources in our anti-TB armament, as well as developing more efficacious drugs, diagnostics, and vaccines. Such a significant reduction in the incidence of TB can occur only by treatment of both active and latent TB cases (2). The emergence and spread of multidrug-resistant (MDR) and extensively drug resistant (XDR) strains of TB poses a serious obstacle to meeting the 2050 goal. Drugs with a novel mechanism of action and chemotherapeutic regimens effective against drug-resistant TB must be developed and tested if we hope to make substantive gains in reducing the worldwide incidence of TB.

Almost 60 years ago, Barry et al. identified clofazimine (CFZ) as a compound that was highly active against *Mycobacterium bovis* Ravanel, as well as *Mycobacterium tuberculosis*, under *in vitro* conditions and in mice following intravenous infection (3). Initial optimism faded, however, when further studies in guinea pigs (4, 5) and nonhuman primates (6) failed to demonstrate significant therapeutic activity, although it should be noted that later studies implicated poor absorption kinetics in these animal models as the primary cause of the lack of efficacy (4). These failures in preclinical animal models, coupled with the identification of the highly effective drug isoniazid and later rifampin, shifted attention away from clinical usage of CFZ to treat TB, although it has been used successfully to treat leprosy since the early 1960s. However, the desire to shorten the duration of treatment necessary to prevent relapse and the emergence of MDR and XDR TB have renewed interest in both CFZ and other related riminophenazine compounds for the treatment of pulmonary tuberculosis (7–9). A recent observational study in Bangladesh examined six combination regimens for efficacy against MDR TB (10). Although all of the regimens contained CFZ during the intensive phase, the two regimens with the highest rate of cure also contained CFZ during the continuation phase. Similarly encouraging results were observed in BALB/c mice (11), demonstrating that the addition of CFZ to a 9-month second-line regimen significantly increased the rate of killing and decreased the relapse rate to levels comparable to that observed in the study by Van Deun et al. (10). CFZ has also recently been shown to have significant additive activity in BALB/c mice when administered with bedaquiline (TMC207) and pyrazinamide (12, 13). Therefore, the addition of CFZ to novel TB drug regimens may augment efforts to shorten the duration of TB chemotherapy, which is the ultimate goal of the Global Alliance for TB Drug Development and the Critical Path to TB Drug Regimens initiative (14).

CFZ is a poorly soluble, lipophilic drug that is highly protein bound and possesses an exceptionally long half-life of approximately 70 days in mice (15). The drug partitions to adipose tissue, and due to its relative insolubility, it preferentially accumulates within macrophages (16, 17) and is known to have immunosuppressive properties (18). As a result of the highly elongated pharmacokinetic/pharmacodynamic profile, CFZ can accumulate to very high levels within tissues and can crystallize within cells, especially in the gastrointestinal tract. In addition, long-term use can result in coloration of the skin that while medically unimportant can cause social stigmatization. Efforts are under way to syn-

Received 10 March 2014 Returned for modification 3 April 2014
Accepted 26 April 2014
Published ahead of print 5 May 2014
Address correspondence to Anne J. Lenaerts, anne.lenaerts@colostate.edu.

doi:10.1128/AAC.02565-14

thesize and test CFZ analogs to find compounds with reduced side effects and more favorable pharmacodynamic properties (8, 9).

While many important insights have been gained from mouse models of TB infection, the discordance between the histological appearance of human and mouse pulmonary granulomas limits the practical usefulness of the mouse when modeling aspects such as drug penetration of fibrotic and caseous necrotic lesions, activity within hypoxic microenvironments, and activity against bacilli under different metabolic conditions. In addition, the bacilli within human pulmonary granulomas, especially those involved in cavitary disease and transmission, are believed to be primarily extracellular (19). However, the bacilli within the lungs of traditional mouse models of infection are predominantly intracellular (20). Therefore, the efficacy of compounds that preferentially accumulate within macrophages could be overestimated by testing in an animal model that lacks necrotic lesions containing abundant extracellular bacilli.

Igor Kramnik's group discovered that the C3HeB/FeJ mouse strain (commonly referred to as the Kramnik mouse model) was highly susceptible to infection with *M. tuberculosis* (21). They also determined that this increased susceptibility was mediated to a large degree by functional inactivation due to naturally occurring mutations in the intracellular pathogen resistance 1 (*Ipr1*) isoform of the interferon-inducible 75 (*Ifi75*) gene (22). Interestingly, following experimental aerosol infection, this mouse strain developed large, caseating granulomas in the lung that have been shown by our group and others to be hypoxic (23, 24). These granulomas contain large numbers of extracellular bacilli and are often surrounded by a rim of foamy macrophages harboring intracellular bacilli (23). Over time, many of these granulomas show evidence of continuous collagen remodeling and fibrotic encapsulation (23). These granulomas bear a striking resemblance to human pulmonary lesions and may facilitate more realistic modeling of microenvironmental conditions not found within conventional mouse models.

Due to renewed interest in use of CFZ as an adjunct to novel chemotherapeutic regimens, we wanted to assess the efficacy of this drug in the Kramnik mouse model of infection to determine if CFZ is effective against extracellular bacteria, under hypoxic conditions, and against bacterial phenotypes exposed to environmental conditions believed to be more similar to what tubercle bacilli experience in human lung lesions.

MATERIALS AND METHODS

Animals. Female specific-pathogen-free C3HeB/FeJ and BALB/c mice, ages 6 to 8 weeks, were purchased from Jackson Laboratories, Bar Harbor, ME. Mice were housed in a biosafety level III animal facility and maintained with sterile bedding, water, and mouse chow. Specific-pathogen-free status was verified by testing sentinel mice housed within the colony for 13 known mouse pathogens.

Bacteria and aerosol infections. The *M. tuberculosis* Erdman strain (TMCC 107) was used for aerosol infections of mice for drug evaluations and prepared as previously described (25, 26). Briefly, the bacteria were originally grown as a pellicle to generate low-passage-number seed lots (25). Working stocks were generated by growing to mid-log phase in Proskauer-Beck medium containing 0.05% Tween 80 (Sigma-Aldrich, St. Louis, MO) in three passages, enumerated by serial dilution on 7H11 agar plates, divided into 1.5-ml aliquots, and stored at −80°C until use.

C3HeB/FeJ mice and BALB/c mice were exposed to a low-dose aerosol infection with *M. tuberculosis* in a Glas-Col inhalation exposure system, as previously described (26). The inoculum concentration was adjusted to yield ~50 to 75 CFU or ~400 CFU in the lungs of C3HeB/FeJ mice or BALB/c mice, respectively. Five mice were sacrificed on the following day to determine the number of CFU implanted in the lungs.

Drug treatment and enumeration of bacterial load in lungs and spleens. For drug-treated animals, CFZ (Sigma-Aldrich) was prepared by grinding with a mortar and pestle and added to 0.05% agarose dissolved in sterile distilled water. Individual animals were administered a 200-μl dose at 20 mg/kg of body weight daily for 5 days a week via oral gavage. For CFZ-treated animals, treatment was initiated either 3, 4, or 7 weeks following aerosol infection. Mice were euthanized after 2, 4, and 8 weeks of treatment by CO_2 inhalation. At the time of sacrifice, all lung lobes and the spleens were aseptically removed and disrupted with a tissue homogenizer (Glas-Col Inc., Terra Haute, IN) in 4 ml of phosphate-buffered saline (PBS). The number of viable organisms was determined by plating serial dilutions of lung homogenate on Middlebrook 7H11 agar plates supplemented with oleic acid-albumin-dextrose-catalase (OADC) (Gibco BRL, Gaithersburg, MD), 0.03 mg/ml cycloheximide, and 0.05 mg/ml carbenicillin. Due to the long half-life and high protein binding capacity of CFZ, lungs and spleens from drug-treated animals were homogenized in saline plus 10% bovine serum albumin (BSA) and plated on 7H11-OADC agar plates containing 0.4% activated charcoal to prevent carry-over (12). Colonies were counted after at least 21 days of incubation at 37°C and at least 42 days for charcoal-containing plates (26). The viable bacterial counts of whole organs were calculated and converted to logarithms [CFU counts were log transformed as $\log_{10}(x + 1)$, where x equals the total organ CFU count]. The data were expressed as the mean $\log_{10}$ CFU ± the standard error of the mean for each group.

***In vitro* bacterial cultivation.** All *in vitro* cultivation of *M. tuberculosis* Erdman was performed in Dubos Tween-albumin (DTA) medium (27) in sterile 20-mmby 12-mm glass screw-cap tubes containing 12-mmby 4-mm stir bars. Cultures were grown aerobically with high (aerobic) or low (hypoxic) aeration or under anoxic conditions using the rapid anaerobic dormancy (RAD) model, as described by Leistikow et al., where bacterial metabolism drives the oxygen concentration to undetectable levels, utilizing rapid stirring, a small headspace volume, and tightly sealed screw-cap tubes (28). For aerobic growth under high and low aeration, cultures were diluted to an optical density at 600 nm (OD_{600}) of 0.05 and inoculated into sterile 20-mm by 125-mm glass screw-cap tubes containing 12-mm by 4-mm stir bars at final volumes of 1 ml and 10 ml for high and low aeration, respectively. The 10-ml culture has a 10-fold-lower surface-to-volume ratio than the 1-ml high-aeration culture. Cultures were given either CFZ at a final concentration of 50 μg/ml or dimethyl sulfoxide (DMSO) as a vehicle control, sealed with loose-fitting caps, and incubated at 37°C with rapid stirring. The MIC was previously determined to be 0.24 μg/ml for broth and 0.03 μg/ml for 7H11 agar plates for this strain. One, three, and five days later, bacterial cultures were serially diluted in DTA and plated on Dubos agar plates plus OADC and 0.4% activated charcoal. Colonies were counted after at least 21 days of incubation at 37°C.

Statistical analysis. The viable CFU counts were converted to logarithms, which were then evaluated by a one-way analysis of variance, followed by a multiple-comparison analysis of variance by a one-way Tukey test (SAS software program; SAS, Research Triangle Park, NC). Differences were considered significant at the 95% level of confidence.

Pathology and microscopy. All lung lobes from individual mice were collected at necropsy and infused with 4% paraformaldehyde in PBS. Tissue sections were embedded in paraffin and cut to 5-μm thickness on a microtome. Subsequent tissue sections were mounted on glass slides, deparaffinized, and stained with hematoxylin and eosin (H&E). Sections were visualized using a Nikon TE-I motorized microscope controlled by the Nikon NIS Elements software program (Nikon, Melville, NY).

RESULTS

CFZ was highly effective in the lungs of BALB/c but not C3HeB/FeJ mice. BALB/c and Kramnik mice were aerosol infected with

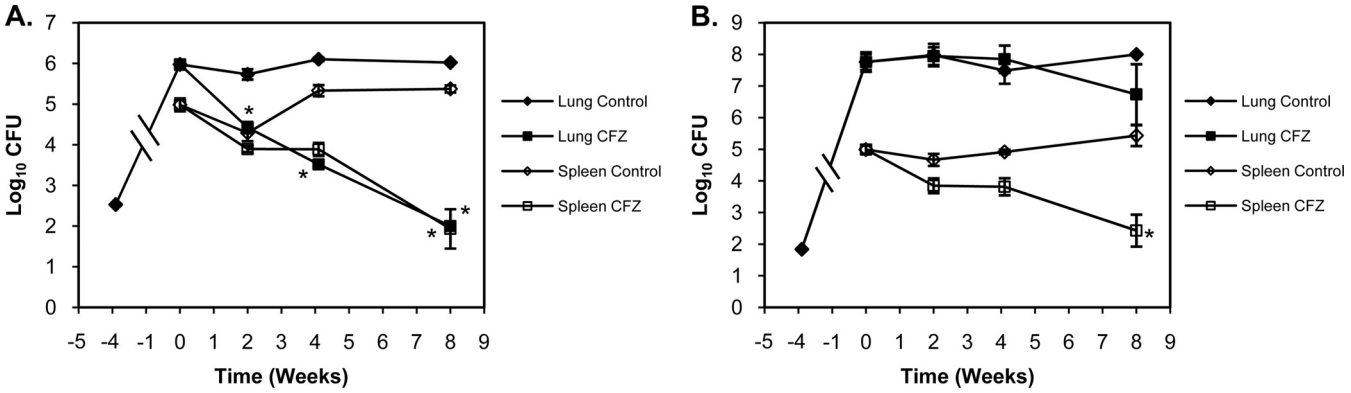

FIG 1 CFZ was highly effective at reducing bacterial CFU in BALB/c mice (A) in the lungs (filled symbols) and in the spleen (open symbols). In contrast, CFZ activity was significantly attenuated in the lungs of C3HeB/FeJ mice (B), while comparable activity was observed in the spleen. Data represent mean $\log_{10}$ CFU counts ± SEM; detection limit = 50 CFU. *, $P < 0.001$.

2.53 ± 0.03 $\log_{10}$ CFU and 1.8 ± 0.03 $\log_{10}$ CFU, respectively. After 4 weeks, bacterial loads in the lungs reached 6.0 $\log_{10}$ CFU in BALB/c mice and 7.8 $\log_{10}$ CFU in Kramnik mice, at which point mice in treatment groups were administered 20 mg/kg CFZ via oral gavage 5 days per week. Treatment with CFZ was highly effective in the lungs of BALB/c mice (Fig. 1A), producing a continuous and progressive decline, culminating in a 2.5-$\log_{10}$ CFU reduction in bacterial numbers after 4 weeks of treatment ($P < 0.001$). Pulmonary bacterial numbers continued to decline in BALB/c mice, ultimately reaching 2.0 $\log_{10}$ CFU, which amounted to a 4.0-$\log_{10}$ CFU reduction after 8 weeks of CFZ treatment.

In contrast to BALB/c mice, Kramnik mice treated with CFZ for 4 weeks showed no decrease in pulmonary CFU (Fig. 1B). Although 8 weeks of treatment resulted in a 1.0-$\log_{10}$ CFU decrease in bacterial numbers, this decrease was not statistically different from results for control (untreated) Kramnik mice at this time point.

CFZ treatment of BALB/c mice was also highly effective at reducing bacterial numbers in the spleen, ultimately achieving a 3.1-$\log_{10}$ CFU reduction after 8 weeks of treatment ($P < 0.001$). Of importance, CFZ treatment was also highly effective at reducing bacterial numbers in the spleens of Kramnik mice. Eight weeks of CFZ treatment resulted in a 2.6-$\log_{10}$ CFU reduction, which was comparable to that observed in the spleens of BALB/c mice ($P > 0.05$).

The pathological progression of granuloma formation in Kramnik mice. The strikingly different pathological progression of disease in the lungs of Kramnik mice in comparison to that in BALB/c mice is likely responsible for the differential response to CFZ between these two strains of mice. To further understand the role that the pathological process of granuloma formation played in the observed attenuation of CFZ efficacy, we performed a comprehensive histological analysis to understand the pathological progression of granuloma development in the lungs of Kramnik mice to identify a time point prior to the formation of well-developed caseous necrotic granulomas and a time point where we reproducibly observed such well-developed granulomas.

At 3 weeks postinfection, the inflammatory lesions in the lungs of BALB/c mice were characterized as loosely organized cellular aggregates composed of macrophages, epithelioid macrophages, and large numbers of lymphocytes that were primarily localized within perivascular regions (Fig. 2A), consistent with observations of Rhoades et al. (29). Small isolated pockets of neutrophils were only occasionally observed. Kramnik mice exhibited markedly different cellular lesions composed predominantly of neutrophilic clusters interspersed with epithelioid macrophages (Fig. 2B). Few if any lymphocytes were found within these lesions. At this time point, only small foci of individual cellular necrosis were present in the lungs of Kramnik mice, and large lesions containing caseous necrotic material were absent.

By 7 weeks of infection, the pulmonary lesions in BALB/c mice were predominantly composed of multifocal coalescing lesions. These lesions were composed of disorganized clusters of macrophages, epithelioid macrophages, and increasing numbers of foamy macrophages surrounded by large numbers of lymphocytes arranged as punctate clusters in association with epithelioid and foamy macrophages (Fig. 2C). In contrast, the lesions in the lungs of Kramnik mice progressed to highly organized structures, which consistently displayed large areas of central caseous necrosis and a peripheral rim of foamy macrophages, with or without a well-defined collagen rim (Fig. 2D).

Highly organized granulomas and caseous necrosis were not observed in the spleens of BALB/c mice (Fig. 2E) or Kramnik mice (Fig. 2F), even though bacterial numbers in the spleens of both mouse strains were comparable.

Pulmonary pathology was responsible for the differential effectiveness of CFZ. To determine the impact of the granuloma pathology upon the effectiveness of drug treatment with CFZ, Kramnik mice were infected with a low-dose aerosol (LDA), and CFZ treatment was initiated prior to the formation of well-defined granulomas (3 weeks postinfection) or after the formation of caseous necrotic granulomas (7 weeks postinfection). Three weeks following infection, bacterial loads in the lungs of Kramnik mice reached 7.1 ± 0.11 $\log_{10}$ CFU (Fig. 3A). Four weeks of CFZ treatment reduced the pulmonary bacterial load in Kramnik mice by 5.8 $\log_{10}$ CFU ($P < 0.001$). Seven weeks after infection, bacterial loads reached 7.7 ± 0.36 $\log_{10}$ CFU. However, treatment with CFZ for 4 weeks after the development of extensive pulmonary pathology only resulted in a 1.6-$\log_{10}$ CFU reduction in the lungs of Kramnik mice.

In the spleens of Kramnik mice where no necrotic granulomas were observed at all time points tested, bacterial loads reached 3.7 ± 0.11 $\log_{10}$ CFU 3 weeks after aerosol infection (Fig. 3B). In response to 4 weeks of CFZ treatment initiated after 3 weeks of

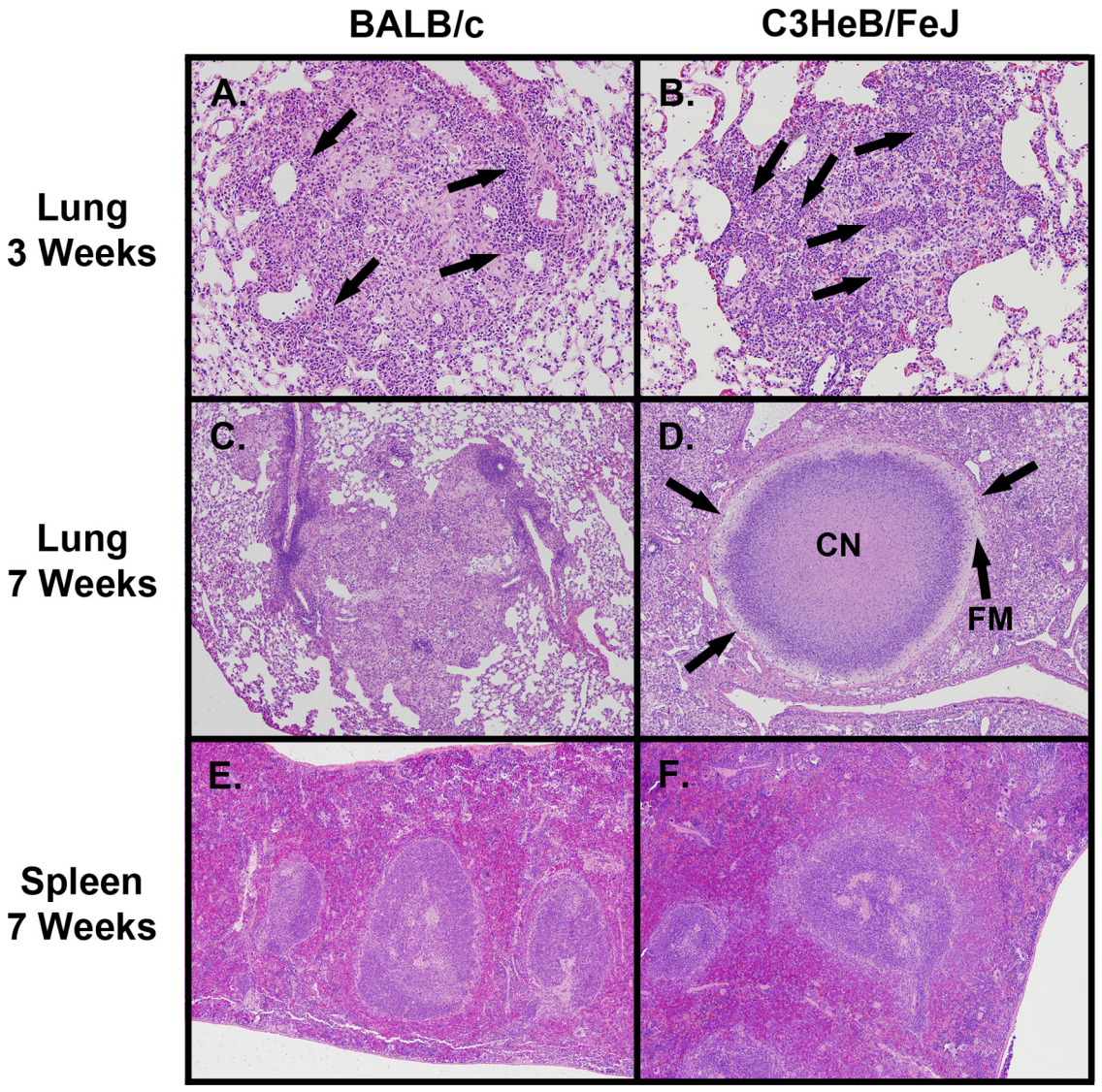

FIG 2 Pathological progression of disease in BALB/c and C3HeB/FeJ mice. Cellular aggregates in the lungs of BALB/c mice at 3 weeks postinfection (A) (magnification, ×100) were composed predominantly of macrophage cells with distinct regions of lymphocytic perivascular and peribronchiolar cuffing (arrows). C3HeB/FeJ mice at 3 weeks postinfection (B) (×100) exhibited cellular lesions composed predominantly of neutrophilic clusters (arrows) and epithelioid macrophages, with evidence of an early fibrotic response. By 7 weeks (C) (×40), the cellular aggregates in BALB/c mice formed loosely organized inflammatory granulomas lacking a well-defined collagen rim. In contrast, by 7 weeks (D) (×40), highly organized granulomas had formed in the lungs of C3HeB/FeJ mice possessing a hypoxic neutrophilic central caseous necrotic core region (CN) and a layer of foamy macrophages (FM) delineated by a collagen rim (arrows) that encapsulated the granuloma structure. By 7 weeks postinfection, no caseating necrotic granulomas were observed in the spleens of BALB/c (E) (×40) or C3HeB/FeJ (F) (×40) mice.

infection, bacterial numbers dropped 2.4 $\log_{10}$ CFU. In mice infected for 7 weeks, bacterial loads reached 5.1 ± 0.10 $\log_{10}$ CFU, and treatment with CFZ for 4 weeks resulted in a 1.3-$\log_{10}$ CFU reduction.

CFZ was effective in immunocompromised IFN-γ knockout mice. Since CFZ is known to have immunomodulatory properties, we wanted to ensure that the weakened immune status of the Kramnik mice was not responsible for the lack of CFZ efficacy observed in the lungs. We infected highly susceptible gamma interferon (IFN-γ) knockout (GKO) mice with *M. tuberculosis* via the LDA route. After 13 days, when the bacterial load was 7.1 $\log_{10}$ CFU in the lungs and 4.6 $\log_{10}$ CFU in the spleen, we initiated CFZ monotherapy in the experimental group of animals. After 10 days of treatment, the pulmonary bacterial load decreased by 3.1 $\log_{10}$ CFU (Fig. 4A) and the bacterial load in the spleen decreased by 4.0 $\log_{10}$ CFU in the GKO mice (Fig. 4B). This decrease was comparable to that observed in immunocompetent BALB/c mice (Fig. 1A), indicating that the loss of CFZ activity in the lungs of Kramnik mice was not related to decreased immune function in these animals.

CFZ was ineffective under anaerobic conditions *in vitro*. We next wanted to compare the activity of CFZ under aerobic, hypoxic, and anaerobic conditions to determine the role of oxygen in CFZ activity. CFZ treatment of aerobic cultures (loose cap permitting free air exchange) of *M. tuberculosis* Erdman resulted in a 2.5-$\log_{10}$ CFU reduction by 3 days posttreatment and a 7.3-$\log_{10}$

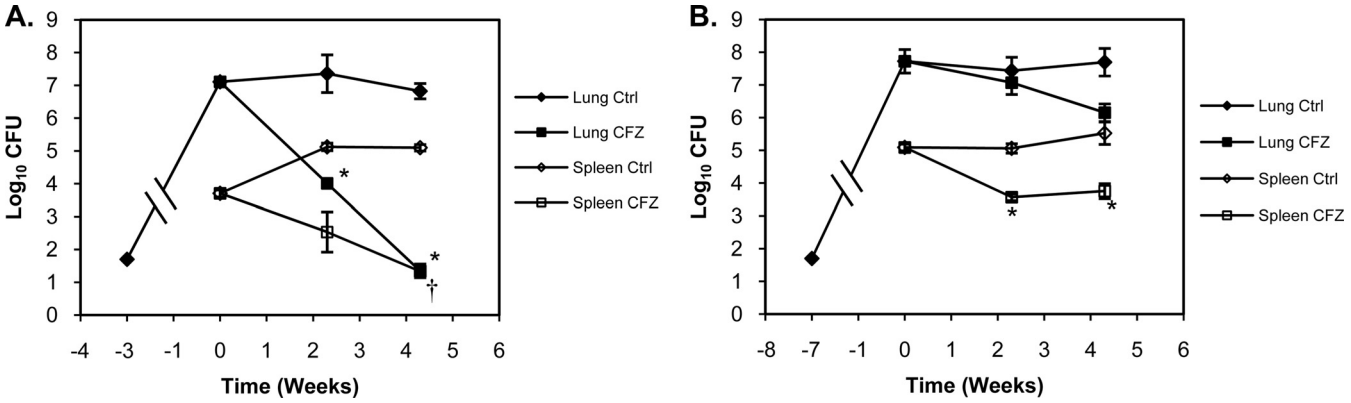

FIG 3 Attenuation of CFZ activity was related to pulmonary pathology. Administration of CFZ to C3HeB/FeJ mice prior to the formation of well-defined pulmonary granulomas (A) (3 weeks postinfection) reconstituted bactericidal activity in the lungs (filled symbols). Initiation of CFZ treatment after the formation of well-defined pulmonary granulomas with significant caseous necrosis (B) (7 weeks postinfection) resulted in significant attenuation of bactericidal activity in C3HeB/FeJ mice. CFZ exhibited comparable activity in the spleens (open symbols) of C3HeB/FeJ mice, which lack well-defined granulomas and caseous necrosis. Data represent mean $\log_{10}$ CFU counts ± SEM; detection limit = 50 CFU. *, $P < 0.001$; †, $P < 0.05$.

CFU reduction after 5 days (Fig. 5A). CFZ activity decreased significantly when *M. tuberculosis* was cultured under hypoxic conditions (1:10 culture volume-to-headspace ratio), with only a 0.92-$\log_{10}$ CFU reduction observed after 3 days and a 2.8-$\log_{10}$ CFU reduction after 5 days (Fig. 5B). We then utilized a derivation of the traditional Wayne model (30) known as the rapid anaerobic dormancy (RAD) model (28) to culture *M. tuberculosis* Erdman under anaerobic conditions. In this culture system, oxygen is completely consumed after 6 days of culture using a 1:10 culture volume-to-headspace ratio. CFZ was administered in an anaerobic chamber at day 12 in the RAD model. After 1 day, a 0.58-$\log_{10}$ reduction in CFU was observed (Fig. 5C), which increased slightly to a 0.90-$\log_{10}$ CFU reduction by 8 days following treatment.

DISCUSSION

Although CFZ has impressive *in vitro* killing kinetics and efficacy in traditional mouse models of TB infection, its lack of efficacy in guinea pigs and rhesus monkeys and its unusual pharmacokinetic properties and high lipophilicity have limited widespread clinical usage for the treatment of pulmonary tuberculosis. A major finding in the studies presented here is that CFZ activity is diminished in a mouse model with caseous necrotic granulomas compared to that in a traditional mouse model. We showed here that CFZ monotherapy was effective against the primarily intracellular bacilli located within the inflammatory lesions in the lungs of BALB/c mice. However, this activity was highly attenuated in the lungs of Kramnik mice possessing hypoxic, caseous necrotic lesions containing primarily extracellular bacilli. In contrast, CFZ was similarly effective in the spleens of both BALB/c and Kramnik mice, suggesting that the lack of CFZ activity observed in the lungs was not due to fundamental differences in pharmacokinetics of the drug in these two mouse strains. Preliminary pharmacokinetic analysis of CFZ showed similar drug levels in plasma for both *M. tuberculosis*-infected BALB/c and Kramnik mice (data not shown).

In order to ensure that the diminished CFZ activity in the lungs was not due to a specific inherent characteristic of the C3HeB/FeJ mouse strain, we showed in a subsequent study using only Kramnik mice that CFZ activity was observed in the lungs at early stages of infection in the absence of caseous necrotic lesions, whereas CFZ activity was highly diminished at time points when lung lesions became necrotic. Again, in contrast to the attenuated efficacy observed in the lungs, CFZ remained effective in the spleens of Kramnik mice throughout all stages of infection, showing *in vivo* efficacy similar to that with BALB/c mice. An examination of the histopathology of the spleen tissue of Kramnik mice failed to show highly organized granulomas with evidence of caseous necrosis at all time points examined, similar to observations made by

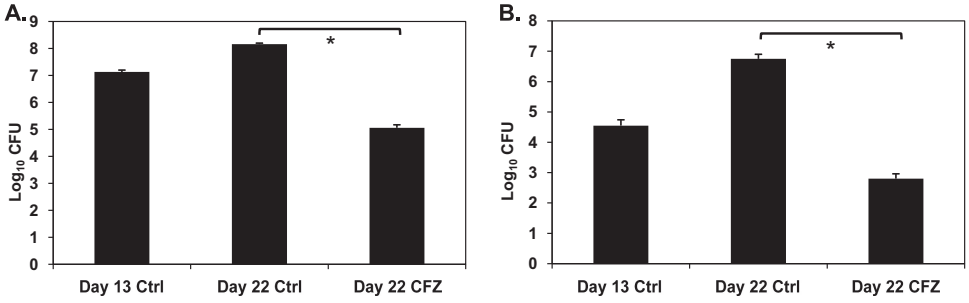

FIG 4 CFZ was effective in immunocompromised GKO mice. Gamma interferon gene-disrupted mice were treated for 9 days with 20 mg/kg CFZ beginning on day 13 postinfection. CFZ reduced bacterial loads in the lungs (A) by 3.1 $\log_{10}$ CFU and in the spleens (B) by 3.95 $\log_{10}$ CFU compared to results for untreated controls. Data represent mean $\log_{10}$ CFU counts ± SEM; detection limit = 50 CFU. *, $P < 0.001$.

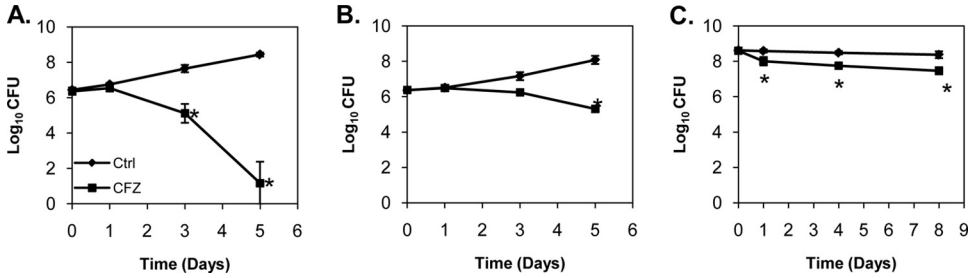

FIG 5 CFZ activity decreased as the oxygen concentration decreased. CFZ was highly effective *in vitro* under high aeration (A). Under low aeration (B), CFZ had reduced but demonstrable activity despite similar bacterial growth. However, CFZ activity was lowest under completely anaerobic conditions achieved in the rapid anaerobic dormancy (RAD) culture model (C). CFZ was added at a final concentration of 50 mg/ml. Data represent mean $\log_{10}$ CFU counts ± SD; detection limit = 50 CFU. *, $P < 0.001$.

Pichugin et al. (31). Therefore, the consistent efficacy of CFZ throughout the course of infection in the spleens of Kramnik mice and the lack of advanced necrotic lesions in this organ further implicate the pathological response as being the predominant factor contributing to the attenuated efficacy of CFZ in the lungs.

Although Kramnik mice are not generally considered immunosuppressed, they nevertheless possess a specific immune defect related to functional inactivation of the *Ipr1* genes (22). Due to the reported immunomodulatory effects of CFZ upon host cells, we wanted to ensure that the weakened immune status of the Kramnik mice was not responsible for the lack of CFZ efficacy in the lungs. CFZ has been shown to have proinflammatory effects, by stimulating the production of superoxide anion (32). CFZ also possesses anti-inflammatory effects, such as inhibition of neutrophil motility and activation of phospholipase A_2 in neutrophils, leading to the production of prostaglandin E_2 and other anti-inflammatory mediators (32–34). In addition to its effect upon neutrophils, CFZ also inhibits the lymphocyte proliferative response to mitogens, which may be related to its binding to the Kv1.3 potassium channel and perturbation of calcium oscillations required for optimal T cell receptor signaling and T cell proliferation (34, 35). In order to ensure that the altered immune status of the Kramnik mouse model was not responsible for the lack of activity of CFZ, we evaluated the drug in the GKO mouse model. Deletion of the gamma interferon gene renders these mice highly susceptible to infection with *M. tuberculosis* by incapacitating the T-helper type 1–IFN-γ axis of *M. tuberculosis* immunity (36). We found that CFZ was highly effective in both the lungs and spleens of GKO mice when administered for 9 days. This efficacy was similar to that observed in BALB/c mice. These results support the idea that the differential activity of CFZ in BALB/c and Kramnik mice is specifically related to the granulomatous pathology in the lungs of these mice and is not due to differences in immune function between mouse strains.

The pathological process resulting in the development of pulmonary granulomas is a highly regulated, coordinated immunological process involving multiple cell types, cytokines, and proinflammatory mediators. It has been hypothesized that the granuloma effectively walls off bacilli residing within an infectious focus, preventing further intrapulmonary and extrapulmonary dissemination (37). Conversely, this structure may also create an environment that facilitates bacterial persistence over long periods of time. Pulmonary granulomas in Kramnik mice have been shown by our group (23) and others (24) to be hypoxic, which may alter bacterial metabolism and promote a state of latency. The highly organized collagen layers surrounding the granuloma may also act as a barrier to immune cells, preventing eradication of the bacilli by host defense mechanisms. Last, this structure may represent a significant barrier to effective drug treatment by impeding drug penetration into mature lesions, resulting in subtherapeutic concentrations of drug within this microenvironment and increasing the likelihood of the emergence of drug resistance.

Although the mechanism of action for CFZ is not entirely clear, the bacterial outer membrane and in particular electron transport are thought to be the primary target. In the original 1957 paper, Barry et al. speculated that the high redox potential of CFZ suggested a mechanism of action where CFZ cycles between oxidized and reduced states, generating reactive oxygen species with antimicrobial activity (3). This hypothesis was supported by recent elegant work from Harvey Rubin's group indicating that CFZ is able to siphon off electrons from the bacterial electron transport chain by competing with the menaquinone pool for electrons donated by NADH to the oxidoreductase NDH-2 (38). In this model, CFZ is reduced upon interaction with NDH-2 and subsequently oxidized in the presence of molecular oxygen in a redox cycle which simultaneously generates superoxide and hydrogen peroxide and depletes intracellular ATP pools. Under hypoxic conditions, reduced availability of oxygen would slow the formation of reactive oxygen species (ROS) and limit the reoxidation of CFZ to its active form. However, recent work by Liu and Imlay (39) and by Keren et al. (40) has cast doubt upon the idea that many antibiotics exert their bactericidal effects through a common mechanism of ROS production. Since the granulomas within the lungs of Kramnik mice have been shown to be hypoxic, the proposed redox mechanism of action for CFZ is at least consistent with our *in vivo* data demonstrating attenuated CFZ activity in the Kramnik model of TB infection after the formation of well-developed, hypoxic granulomas.

To further examine the potential role of molecular oxygen in the attenuation of CFZ activity, we evaluated CFZ activity in *M. tuberculosis* cultures at various oxygen concentrations. For this purpose, we utilized the *in vitro* RAD bacterial culture model to generate hypoxic and completely anaerobic bacterial cultures (28). In this assay, the active metabolism of the bacilli drives the oxygen concentration in the headspace of sealed culture tubes over time to undetectable levels (28). In these studies, CFZ activity decreased significantly when bacteria were cultured under hypoxic conditions, and the activity was further attenuated in the absence of oxygen. These results were somewhat surprising, since other researchers have reported that CFZ had significant antimy-

cobacterial activity using different low-oxygen *in vitro* culture systems (8, 41, 42). In our assay, the loss of oxygen was monitored using methylene blue as an indicator to demonstrate that the cultures were hypoxic (30). In addition, we harvested, manipulated, and plated the cultures under low-oxygen conditions within a sealed container inside the biosafety cabinet to prevent alteration of the bacterial metabolic phenotype. Most other culture systems, such as the low-oxygen recovery assay (LORA), still have small residual amounts of oxygen (<0.16%), which may allow redox cycling of CFZ (albeit at a reduced rate) and some antibacterial activity. Of importance, these very minute amounts of oxygen could be sufficient to preserve CFZ effectiveness. Also, the presence of oxygen during the 28-h recovery phase of the LORA could potentially compromise the results and overestimate the efficacy of CFZ under these conditions. However, it should be noted that even when cultured under completely anaerobic conditions using the RAD model, CFZ still retained ~1 $\log_{10}$ of bactericidal activity (as seen in Fig. 5C), suggesting that other mechanisms in addition to molecular oxygen may potentially contribute to the observed killing. In that respect, we can speculate that other electron donors could be involved in the reduction of CFZ into the active form. Last, in the *in vitro* studies performed here, *M. tuberculosis* Erdman was used, whereas most other investigators used *M. tuberculosis* H37Rv in the LORA and other anaerobic culture systems (8, 41). Strain-specific differences in susceptibility of *M. tuberculosis* to CFZ under low-oxygen conditions are now being further investigated to address this question.

It has been suggested that CFZ has improved activity when bacteria are intracellular due to the accumulation of the drug within immune cells (43, 44). In TB patients with active disease, it is thought that the majority of bacteria are extracellular in various lung compartments (in sputum and in necrotic, fibrotic, and cavitary lung lesions). The pharmacokinetics of the drug are such that CFZ accumulates to high levels in the tissues and within macrophages (45–47), while serum concentrations are low. Together with the high protein binding of CFZ (≥99% plasma protein binding [Anna Upton, personal communication]), this partitioning may limit the exposure of extracellular bacilli to biologically active drug concentrations (48). Of additional importance, the granuloma structure itself may impede drug penetration, preventing exposure of bacilli within caseous necrotic lesions to bactericidal concentrations of drugs and facilitating the emergence of antimicrobial resistance. A recent report by Prideaux et al. demonstrated that moxifloxacin preferentially accumulates in immune cells surrounding the caseum, with decreased penetration into the caseum of necrotic granulomas in a rabbit model of TB infection (49). Experiments are currently in progress to quantify CFZ drug levels and to assess the penetration of CFZ into caseous granulomas in Kramnik mice.

It is important to understand that while CFZ monotherapy showed limited activity in the necrotic lung lesions of Kramnik mice, clinical usage of CFZ would always be in combination with other drugs. Therefore, the results presented in this study should be interpreted with caution. CFZ may still have synergistic effects with other TB drugs and/or a nonoverlapping spectrum of activity targeting subpopulations of bacteria that are difficult to eradicate using available TB drugs. In addition, as lung pathology begins to resolve due to the action of efficacious companion drugs, the changing microenvironment may promote CFZ activity. Studies in our laboratory are under way to investigate the addition of CFZ to combination drug regimens in Kramnik mice.

Our results are in concordance with the recent clinical results for CFZ in a phase IIa early bactericidal activity (EBA) clinical study (NC-003) conducted by the Global Alliance for TB Drug Development. A preliminary analysis of the NC-003 trial (D. Everitt, presented at the Union World Conference on Lung Health, Paris, France, November 2013) showed no efficacy of CFZ monotherapy in the first 14 days of treatment and no additive effect when CFZ was added to bedaquiline and PA-824 (50). Although EBA trials serve as an important starting point to determine appropriate dosing and define short-term clinical efficacy, the results obtained from EBA studies may not completely reflect the total spectrum of killing activity of all drugs (51). Long-term administration (>14 days) of CFZ may still provide significant sterilizing activity that is not evident in an EBA study and may prevent relapse of infection. Of importance, the concentrations of CFZ in plasma that were observed in the trial were significantly lower than mathematical models predicted for that dosing regimen based upon prior data (52), potentially underestimating the CFZ efficacy. Higher doses may be needed to optimize the contribution of CFZ in multidrug regimens.

Another explanation for the inactivity of CFZ may relate to the nature of the bacterial subpopulation(s) found in sputum originating with cavitary lesions, where oxygenation is limited. A better understanding of the metabolic state of bacterial populations in sputum samples would be required to answer that question.

The development of well-defined, hypoxic granulomas with abundant caseous necrosis and extracellular bacilli in Kramnik mice provides a low-cost, convenient animal model to evaluate the impact of such lesions on drug efficacy. Differential activity of CFZ in a traditional BALB/c mouse model and the Kramnik mouse model underscores the utility of the latter model in dissecting further the *in vivo* activity of a drug. Animal models that more accurately reflect the spectrum of pathological complexity within the lung may improve the concordance between preclinical models and human clinical trials.

ACKNOWLEDGMENTS

This work was supported by the Bill and Melinda Gates Foundation under grants 1033596, "Evaluation of a new murine model for testing tuberculosis chemotherapy," and 1037174, "Qualification of C3HeB/FeJ mice for experimental chemotherapy of tuberculosis," and National Institutes of Health grant AI061505.

We acknowledge the staff of the Laboratory Animal Resources at Colorado State University for their animal care. We thank Phil Chapman (Colorado State University) for statistical support and Michael Lyons for helpful discussions.

REFERENCES

1. **Glaziou P, Falzon D, Floyd K, Raviglione M.** 2013. Global epidemiology of tuberculosis. Semin. Respir. Crit. Care Med. **34:**3–16. http://dx.doi.org/10.1055/s-0032-1333467.
2. **Dye C, Glaziou P, Floyd K, Raviglione M.** 2013. Prospects for tuberculosis elimination. Annu. Rev. Public Health **34:**271–286. http://dx.doi.org/10.1146/annurev-publhealth-031912-114431.
3. **Barry VC, Belton JG, Conalty ML, Denneny JM, Edward DW, O'Sullivan JF, Twomey D, Winder F.** 1957. A new series of phenazines (rimino-compounds) with high antituberculosis activity. Nature **179:**1013–1015. http://dx.doi.org/10.1038/1791013a0.
4. **Barry VC, Buggle K, Byrne J, Conalty ML, Winder F.** 1960. Absorption, distribution and retention of the riminocompounds in the experimental animal. Ir. J. Med. Sci. **416:**345–352.

5. **Vischer WA.** 1969. The experimental properties of G 30 320 (B 663)—a new anti-leprotic agent. Lepr. Rev. **40:**107–110.
6. **Schmidt L, Hoffman R, Jolly P.** 1955. Induced pulmonary tuberculosis in the rhesus monkey: its usefulness in evaluating chemotherapeutic agents. Proceedings of the 14th V.A.-A.V. Conference on Tuberculosis, p 226–231. Veterans Administration, Atlanta, GA.
7. **Jagannath C, Reddy MV, Kailasam S, O'Sullivan JF, Gangadharam PR.** 1995. Chemotherapeutic activity of clofazimine and its analogues against Mycobacterium tuberculosis. In vitro, intracellular, and in vivo studies. Am. J. Respir. Crit. Care Med. **151:**1083–1086. http://dx.doi.org/10.1164/ajrccm/151.4.1083.
8. **Lu Y, Zheng M, Wang B, Fu L, Zhao W, Li P, Xu J, Zhu H, Jin H, Yin D, Huang H, Upton AM, Ma Z.** 2011. Clofazimine analogs with efficacy against experimental tuberculosis and reduced potential for accumulation. Antimicrob. Agents Chemother. **55:**5185–5193. http://dx.doi.org/10.1128/AAC.00699-11.
9. **Zhang D, Lu Y, Liu K, Liu B, Wang J, Zhang G, Zhang H, Liu Y, Wang B, Zheng M, Fu L, Hou Y, Gong N, Lv Y, Li C, Cooper CB, Upton AM, Yin D, Ma Z, Huang H.** 2012. Identification of less lipophilic riminophenazine derivatives for the treatment of drug-resistant tuberculosis. J. Med. Chem. **55:**8409–8417. http://dx.doi.org/10.1021/jm300828h.
10. **Van Deun A, Maug AK, Salim MA, Das PK, Sarker MR, Daru P, Rieder HL.** 2010. Short, highly effective, and inexpensive standardized treatment of multidrug-resistant tuberculosis. Am. J. Respir. Crit. Care Med. **182:**684–692. http://dx.doi.org/10.1164/rccm.201001-0077OC.
11. **Grosset JH, Tyagi S, Almeida DV, Converse PJ, Li SY, Ammerman NC, Bishai WR, Enarson D, Trebucq A.** 2013. Assessment of clofazimine activity in a second-line regimen for tuberculosis in mice. Am. J. Respir. Crit. Care Med. **188:**608–612. http://dx.doi.org/10.1164/rccm.201304-0753OC.
12. **Tasneen R, Li SY, Peloquin CA, Taylor D, Williams KN, Andries K, Mdluli KE, Nuermberger EL.** 2011. Sterilizing activity of novel TMC207- and PA-824-containing regimens in a murine model of tuberculosis. Antimicrob. Agents Chemother. **55:**5485–5492. http://dx.doi.org/10.1128/AAC.05293-11.
13. **Williams K, Minkowski A, Amoabeng O, Peloquin CA, Taylor D, Andries K, Wallis RS, Mdluli KE, Nuermberger EL.** 2012. Sterilizing activities of novel combinations lacking first- and second-line drugs in a murine model of tuberculosis. Antimicrob. Agents Chemother. **56:**3114–3120. http://dx.doi.org/10.1128/AAC.00384-12.
14. **Lienhardt C, Raviglione M, Spigelman M, Hafner R, Jaramillo E, Hoelscher M, Zumla A, Gheuens J.** 2012. New drugs for the treatment of tuberculosis: needs, challenges, promise, and prospects for the future. J. Infect. Dis. **205**(Suppl 2)**:**S241–S249.
15. **Banerjee DK, Ellard GA, Gammon PT, Waters MF.** 1974. Some observations on the pharmacology of clofazimine (B663). Am. J. Trop. Med. Hyg. **23:**1110–1115.
16. **McDougall AC.** 1974. Electron microscope studies of the antileprosy drug B663 (clofazimine; Lamprenel). Int. J. Lepr. Other Mycobact. Dis. **42:**1–12.
17. **McDougall AC, Horsfall WR, Hede JE, Chaplin AJ.** 1980. Splenic infarction and tissue accumulation of crystals associated with the use of clofazimine (Lamprene; B663) in the treatment of pyoderma gangrenosum. Br. J. Dermatol. **102:**227–230. http://dx.doi.org/10.1111/j.1365-2133.1980.tb05697.x.
18. **Prinsloo Y, van Rensburg CE, van der Walt R, Anderson R.** 1995. Augmentative inhibition of lymphocyte proliferation by cyclosporin A combined with the riminophenazine compounds clofazimine and B669. Inflamm. Res. **44:**379–385. http://dx.doi.org/10.1007/BF01797865.
19. **Eum SY, Kong JH, Hong MS, Lee YJ, Kim JH, Hwang SH, Cho SN, Via LE, Barry CE, III.** 2010. Neutrophils are the predominant infected phagocytic cells in the airways of patients with active pulmonary TB. Chest **137:**122–128. http://dx.doi.org/10.1378/chest.09-0903.
20. **Hoff DR, Ryan GJ, Driver ER, Ssemakulu CC, De Groote MA, Basaraba RJ, Lenaerts AJ.** 2011. Location of intra- and extracellular M. tuberculosis populations in lungs of mice and guinea pigs during disease progression and after drug treatment. PLoS One **6:**e17550. http://dx.doi.org/10.1371/journal.pone.0017550.
21. **Kramnik I, Demant P, Bloom BB.** 1998. Susceptibility to tuberculosis as a complex genetic trait: analysis using recombinant congenic strains of mice. Novartis Found. Symp. **217:**120–131; discussion, 132–137.
22. **Pan H, Yan BS, Rojas M, Shebzukhov YV, Zhou H, Kobzik L, Higgins DE, Daly MJ, Bloom BR, Kramnik I.** 2005. Ipr1 gene mediates innate immunity to tuberculosis. Nature **434:**767–772. http://dx.doi.org/10.1038/nature03419.
23. **Driver ER, Ryan GJ, Hoff DR, Irwin SM, Basaraba RJ, Kramnik I, Lenaerts AJ.** 2012. Evaluation of a mouse model of necrotic granuloma formation using C3HeB/FeJ mice for testing of drugs against Mycobacterium tuberculosis. Antimicrob. Agents Chemother. **56:**3181–3195. http://dx.doi.org/10.1128/AAC.00217-12.
24. **Harper J, Skerry C, Davis SL, Tasneen R, Weir M, Kramnik I, Bishai WR, Pomper MG, Nuermberger EL, Jain SK.** 2012. Mouse model of necrotic tuberculosis granulomas develops hypoxic lesions. J. Infect. Dis. **205:**595–602. http://dx.doi.org/10.1093/infdis/jir786.
25. **Lenaerts AJ, Gruppo V, Marietta KS, Johnson CM, Driscoll DK, Tompkins NM, Rose JD, Reynolds RC, Orme IM.** 2005. Preclinical testing of the nitroimidazopyran PA-824 for activity against Mycobacterium tuberculosis in a series of in vitro and in vivo models. Antimicrob. Agents Chemother. **49:**2294–2301. http://dx.doi.org/10.1128/AAC.49.6.2294-2301.2005.
26. **Orme IM.** 1996. Immune responses in animal models. Curr. Top. Microbiol. Immunol. **215:**181–196.
27. **Kim TH, Kubica GP.** 1972. Long-term preservation and storage of mycobacteria. Appl. Microbiol. **24:**311–317.
28. **Leistikow RL, Morton RA, Bartek IL, Frimpong I, Wagner K, Voskuil MI.** 2010. The Mycobacterium tuberculosis DosR regulon assists in metabolic homeostasis and enables rapid recovery from nonrespiring dormancy. J. Bacteriol. **192:**1662–1670. http://dx.doi.org/10.1128/JB.00926-09.
29. **Rhoades ER, Frank AA, Orme IM.** 1997. Progression of chronic pulmonary tuberculosis in mice aerogenically infected with virulent Mycobacterium tuberculosis. Tuber. Lung Dis. **78:**57–66. http://dx.doi.org/10.1016/S0962-8479(97)90016-2.
30. **Wayne LG, Hayes LG.** 1996. An in vitro model for sequential study of shiftdown of Mycobacterium tuberculosis through two stages of nonreplicating persistence. Infect. Immun. **64:**2062–2069.
31. **Pichugin AV, Yan BS, Sloutsky A, Kobzik L, Kramnik I.** 2009. Dominant role of the sst1 locus in pathogenesis of necrotizing lung granulomas during chronic tuberculosis infection and reactivation in genetically resistant hosts. Am. J. Pathol. **174:**2190–2201. http://dx.doi.org/10.2353/ajpath.2009.081075.
32. **Krajewska MM, Anderson R, O'Sullivan JF.** 1993. Effects of clofazimine analogues and tumor necrosis factor-alpha individually and in combination on human polymorphonuclear leukocyte functions in vitro. Int. J. Immunopharmacol. **15:**99–111. http://dx.doi.org/10.1016/0192-0561(93)90086-E.
33. **Anderson R, Lukey P, Van Rensburg C, Dippenaar U.** 1986. Clofazimine-mediated regulation of human polymorphonuclear leukocyte migration by pro-oxidative inactivation of both leukoattractants and cellular migratory responsiveness. Int. J. Immunopharmacol. **8:**605–620. http://dx.doi.org/10.1016/0192-0561(86)90033-0.
34. **van Rensburg CE, Gatner EM, Imkamp FM, Anderson R.** 1982. Effects of clofazimine alone or combined with dapsone on neutrophil and lymphocyte functions in normal individuals and patients with lepromatous leprosy. Antimicrob. Agents Chemother. **21:**693–697. http://dx.doi.org/10.1128/AAC.21.5.693.
35. **Ren YR, Pan F, Parvez S, Fleig A, Chong CR, Xu J, Dang Y, Zhang J, Jiang H, Penner R, Liu JO.** 2008. Clofazimine inhibits human Kv1.3 potassium channel by perturbing calcium oscillation in T lymphocytes. PLoS One **3:**e4009. http://dx.doi.org/10.1371/journal.pone.0004009.
36. **Flynn JL, Chan J, Triebold KJ, Dalton DK, Stewart TA, Bloom BR.** 1993. An essential role for interferon gamma in resistance to Mycobacterium tuberculosis infection. J. Exp. Med. **178:**2249–2254. http://dx.doi.org/10.1084/jem.178.6.2249.
37. **Saunders BM, Cooper AM.** 2000. Restraining mycobacteria: role of granulomas in mycobacterial infections. Immunol. Cell Biol. **78:**334–341. http://dx.doi.org/10.1046/j.1440-1711.2000.00933.x.
38. **Yano T, Kassovska-Bratinova S, Teh JS, Winkler J, Sullivan K, Isaacs A, Schechter NM, Rubin H.** 2011. Reduction of clofazimine by mycobacterial type 2 NADH:quinone oxidoreductase: a pathway for the generation of bactericidal levels of reactive oxygen species. J. Biol. Chem. **286:**10276–10287. http://dx.doi.org/10.1074/jbc.M110.200501.
39. **Liu Y, Imlay JA.** 2013. Cell death from antibiotics without the involvement of reactive oxygen species. Science **339:**1210–1213. http://dx.doi.org/10.1126/science.1232751.
40. **Keren I, Wu Y, Inocencio J, Mulcahy LR, Lewis K.** 2013. Killing by bactericidal antibiotics does not depend on reactive oxygen species. Science **339:**1213–1216. http://dx.doi.org/10.1126/science.1232688.
41. **Cho SH, Warit S, Wan B, Hwang CH, Pauli GF, Franzblau SG.** 2007.

Low-oxygen-recovery assay for high-throughput screening of compounds against nonreplicating Mycobacterium tuberculosis. Antimicrob. Agents Chemother. **51:**1380–1385. http://dx.doi.org/10.1128/AAC.00055-06.
42. **Xu J, Lu Y, Fu L, Zhu H, Wang B, Mdluli K, Upton AM, Jin H, Zheng M, Zhao W, Li P.** 2012. In vitro and in vivo activity of clofazimine against Mycobacterium tuberculosis persisters. Int. J. Tuberc. Lung Dis. **16:**1119–1125. http://dx.doi.org/10.5588/ijtld.11.0752.
43. **Barry V.** 1964. The development of chemotherapeutic agent for tuberculosis, p 46–64. *In* Barry V (ed), Chemotherapy of tuberculosis. Butterworth & Co., London, England.
44. **Barry VC, Conalty ML.** 1965. The antimycobacterial activity of B 663. Lepr. Rev. **36:**3–7.
45. **Aplin RT, McDougall AC.** 1975. Identification of crystals of the riminophenazine compound B663 (Lamprene: clofazimine) in mouse spleen macrophages by thin layer chromatography and mass spectrum analysis. Experientia **31:**468–469. http://dx.doi.org/10.1007/BF02026384.
46. **Baik J, Rosania GR.** 2012. Macrophages sequester clofazimine in an intracellular liquid crystal-like supramolecular organization. PLoS One **7:**e47494. http://dx.doi.org/10.1371/journal.pone.0047494.
47. **Sandler ED, Ng VL, Hadley WK.** 1992. Clofazimine crystals in alveolar macrophages from a patient with the acquired immunodeficiency syndrome. Arch. Pathol. Lab. Med. **116:**541–543.
48. **Reddy VM, O'Sullivan JF, Gangadharam PR.** 1999. Antimycobacterial activities of riminophenazines. J. Antimicrob. Chemother. **43:**615–623. http://dx.doi.org/10.1093/jac/43.5.615.
49. **Prideaux B, Dartois V, Staab D, Weiner DM, Goh A, Via LE, Barry CE, III, Stoeckli M.** 2011. High-sensitivity MALDI-MRM-MS imaging of moxifloxacin distribution in tuberculosis-infected rabbit lungs and granulomatous lesions. Anal. Chem. **83:**2112–2118. http://dx.doi.org/10.1021/ac1029049.
50. **Global Alliance for TB Drug Development.** 2013. Evaluation of early bactericidal activity in pulmonary tuberculosis with clofazimine, TMC207, PA-824, pyrazinamide (NC-003); NCT01691534. http://clinicaltrials.gov/ct2/show/NCT01691534.
51. **Donald PR, Diacon AH.** 2008. The early bactericidal activity of antituberculosis drugs: a literature review. Tuberculosis (Edinb.) **88**(Suppl 1)**:**S75–S83. http://dx.doi.org/10.1016/S1472-9792(08)70038-6.
52. **Schaad-Lanyi Z, Dieterle W, Dubois JP, Theobald W, Vischer W.** 1987. Pharmacokinetics of clofazimine in healthy volunteers. Int. J. Lepr. Other Mycobact. Dis. **55:**9–15.